GOSPODARKA SUROWCAMI MINERALNYMI – MINERAL RESOURCES MANAGEMENT

2022 Volume 38 Issue 4 Pages 91–104

DOI: 10.24425/gsm.2022.144095

JACEK MISIAK[1]

Geological exploration of the Moon

Introduction

The geological structure of the Moon and its potential resources have been of interest to many researchers for many years. Exploration is difficult due to the significant distance of the research object from Earth (384,400 km). Information on this topic was obtained from multidirectional studies. The oldest studies were based on telescopic observations of the moon; meteorites with material from the lunar surface were also analyzed. As technology progressed, observations were made using lunar satellites and different remote sensing techniques such as multispectral imaging, thermal imaging, radar, gamma-ray spectroscopy, thermal neutrons, epithermal neutrons, fast neutrons, and X-ray spectroscopy. The next step was to send several types of unmanned research probes to the Moon, which were used for in-situ surveys (Luna program – USSR, Surveyor program – US). The first manned mission landed on the Moon on 20 July 1969. This was the Apollo 11 mission, followed by the subsequent successful landings of Apollo 12, 14, 15, 16, and 17 which took place on

✉ Corresponding Author: Jacek Misiak; e-mail: misiak@agh.edu.pl

[1] AGH University of Science and Technology, Faculty of Geology, Geophysics and Environment Protection, Kraków, Poland; ORCID iD: 0000-0002-0708-728X; Scopus ID: 14044125300; Researcher ID: A-7934-2017; e-mail: misiak@agh.edu.pl

11 December 1972 and was the last manned landing to date. In recent years, research has been carried out using unmanned missions such as (Clementine 1994; Lunar Prospector 1998; Chandrayaan-1 2008; Lunar Reconnaissance Orbiter 2009), Lunar Crater Observation and Sensing Satellite (LCROSS 2009). The Chinese automated Moon surface sampling probe landed on the Moon on 1st December 2020. Data obtained in this way make it possible to draw conclusions about the evolution and geological structure of the moon, endogenous processes, phenomena occurring on its surface and the atmospheric conditions prevailing there. From the economic point of view and in the context of the possibility of colonizing the Moon, the exploration of lunar resources is a very important issue. The increasing demand for mineral resources and their limited supply on Earth force us to increasingly look to the Moon and other more distant space objects such as Mars and asteroids.

1. Geology of the Moon

1.1. The surface and subsurface of the Moon

The exploration of the Moon has so far provided a lot of information about the lunar surface and the underlying strata.

Regolith

The top layers are made of a material called regolith (Shoemaker and Hackman 1962; Shoemaker et al. 1967). The regolith is generally thinner than 5–6 m in maria areas and thicker in terrae areas (Shoemaker and Morris 1970; Cooper et al. 1974). The term “soil” is commonly used as a synonym for regolith or to refer to a fine surface material.

Bedrock

The lunar maria are composed of basalt and have a density of 3.3 to 3.4 g/cm^3. Mare basalts typically extend hundreds of meters below the surface and locally reach depths of around 5 km. By contrast, feldspar (plagioclase-rich) bedrock dominates in plains and terrae; feldspar has a lower density of 2.90 to 3.05 g/cm^3. Seismic data indicate that the terra material forms a crust with a thickness of 45 to 75 km (Toksoz et al. 1974). The mean elevations relative to the center of mass of the Moon on the far side are higher than on the nearside (Kaula et al. 1974; Bills and Ferrari 1977). The thickness of the cover can reach up to 120 km under some elevated areas on the other side (the far side of the Moon).

Basins are older than maria (Baldwin 1949, 1978). Stratigraphic observations prove that the maria are filled volcanically and the basins are of impact origin. Mare structures identified as basalt by their dark color and distinctive landforms are superimposed on the impact structures of the basins.

Craters

Lunar craters are mostly of impact origin; a few craters of endogenous origin have also been found. The number of craters present in an area is proportional to the age of the area (Baldwin 1949, 1963; Opik 1960). Small craters are always more abundant than large craters and their distribution is random. The craters were formed by high-velocity space rocks, the size of which ranges from dust particles to small asteroids. Younger craters are superimposed on older craters, which often causes their shapes to be blurred and not very visible.

Lithostratigraphy

El-Baz (El-Baz 1975) developed a lunar stratigraphic sequence and divided it into five recognizable systems: Pre-Nectarian and Nectarian systems – repeated impacts causing large basins and crater formation; Imbrian system – the formation of older basalts; Eratosthenian system – the formation of impact craters in highlands and maria; Copernican system – the formation of smaller craters. The correlation of the Moon's lithostratigraphy compared to the Earth's geological structure and the dominant processes of the Moon formation are shown in Figure 1.

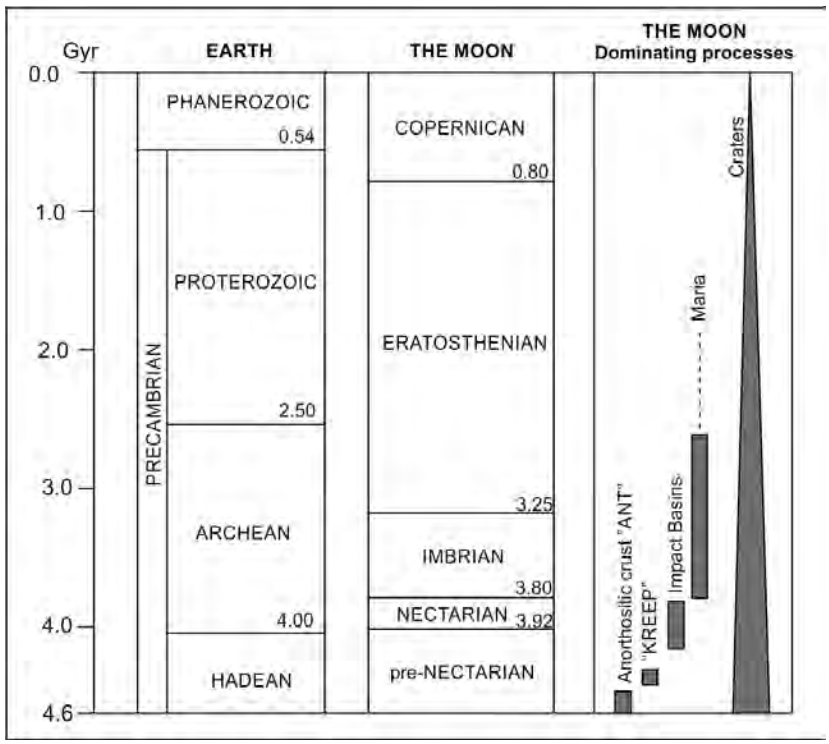

Fig. 1. Simplified lithostratigraphy of the Moon compared to the geological structure of the earth based on: Wilhelms 1987; Neukum and Ivanov 1994; Stöffler and Ryder 2001; van Gasselt and Neukum 2011

Rys. 1. Uproszczona litostratygrafia Księżyca na tle budowy geologicznej Ziemi

The distribution of the various geological outcrops on the Moon is shown on maps based on the United States Geological Survey (USGS) and the NASA Planetary Data System (PDS) data available at: https://astrogeology.usgs.gov/search/map/Moon/Geology/Unified_Geologic_Map_of_the_Moon_GIS_v2 (QGIS and ArcGIS shapefiles). The maps are also available in pdf format in a publication by Fortezzo et al. (2020). *Release of the Digital Unified Global Geologic Map of the Moon At 1:5,000,000- Scale.* Paper presented at the 51st Lunar and Planetary Science Conference, Lunar and Planetary Institute, Houston, TX.

Pre-Nectarian

Pre-Nectarian system: units, description, and interpretation (based on Unified Geologic Map of the Moon (1:5,000,000 scale) after Fortezzo et al. 2020, Figure 2a.

pNb; pre-Nectarian Basin; subdued, eroded mountain rings and arcuate segments of rings, rim, walls, and inner-ring materials; erosionally degraded impact-related structures and ejecta materials.

pNbm; pre-Nectarian Basin Massif; large mountainous landforms, usually lying along the arc, both continuous and discontinuous, gradational and with finer-scale topography. Bedrock uplifted during the formation of basins.

pNc; pre-Nectarian Crater; discontinuous, subdued rim crests and rounded curved, or straight rim remnants; erosionally degraded morphology and material resulting from a primary impact event.

pNt; pre-Nectarian Terra; rugged, diverse terrain, degraded partial crater rims, gradational with smoother Nt unit and rougher pNbm and pNc units; a complex mixture of local erosional debris and crater and basin ejecta; megaregolith.

Nectarian

Nectarian system: units, description, and interpretation (based on Unified Geologic Map of the Moon (1:5,000,000 scale) after Fortezzo et al. 2020, Figure 2a.

Nc; Nectarian Crater; significantly muted topographic relief when compared to younger impact features; broad flat floors (typically another unit), and little to no ejecta present; muted morphology and material from a primary impact event.

Nb; Nectarian Basin, undivided; material of raided walls, slumped blocks of basins, and aggregates of closely spaced subdued hills and ridges; impact-related structures and ejecta material.

Nbl; Nectarian Basin, Lineated; sharp, raised ridges, intervening flat areas or deep troughs and smooth hills with narrow grooves; bedrock pervasively faulted by Imbrium impact.

Nbm; Nectarian Basin, Massif; rugged blocks usually 10 to 30 km across; forms the highest and most rugged parts of arcuate raised ridges; bedrock uplifted during the formation of Nectarian basins.

Nbsc; Nectarian Basin, Secondary Crater; grouped in clusters, chains, and groove-like chains, mostly peripheral and approximately radial to Nectarian basins; secondary impact craters of Nectarian basins.

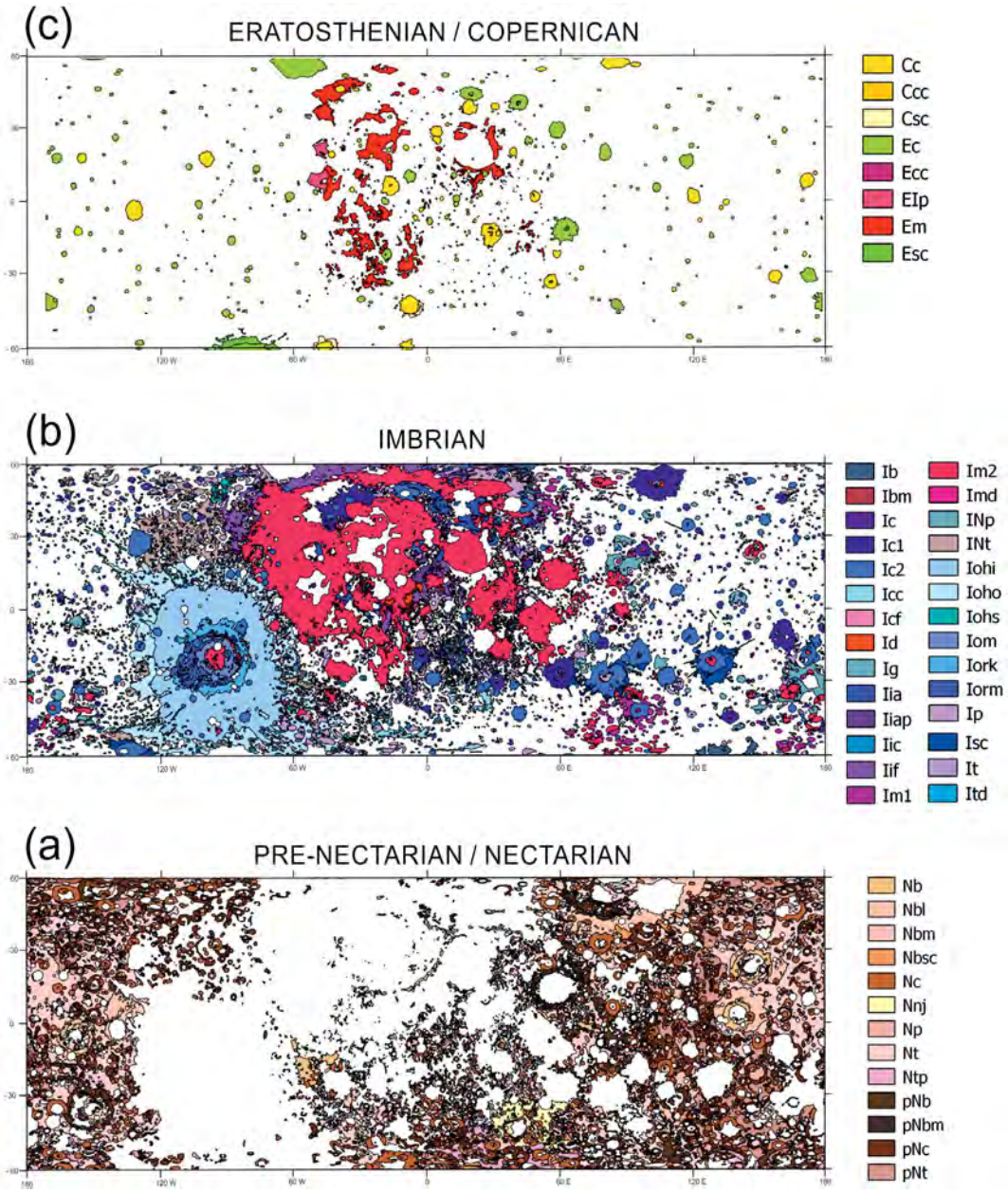

Fig. 2. Distribution of individual geological units on the Moon
(a) Pre-Nectarian and Nestarian systems, (b) Imbrian system,
(c) Eratosthenian and Copernican systems
after: United States Geological Survey (USGS), NASA Planetary Data System (PDS), Fortezzo et al. 2020

Rys. 2. Rozmieszczenie poszczególnych jednostek geologicznych na Księżycu
(a) układy przednektariańskie i nestariańskie, (b) system imbryjski,
(c) system erastotenowski i kopernikański

Nnj; Nectarian Nectaris Janssen Formation; rolling subdued terrain having numerous linear features like ridges, scarps, and grooves radial to the Nectaris basin; Nectaris basin ejecta equivalent to, but more degraded than, units Iif, Iohi, and Ioho.

Np.; **Nectarian Plains**; usually flat, moderate albedo terrain with a dense population of large, old craters; ambiguous origin, possible ejecta from large impacts and basin-forming events.

Nt; Nectarian Terra; relatively rough surface, rolling to moderately rugged overall relief; diverse ages of superposed and buried craters; a complex mixture of local erosional debris and crater and basin ejecta; megaregolith.

Ntp; Nectarian Terra-Mantling and Plains; light colored, wavy or rolling surfaces more heavily cratered than unit Ip; primary and secondary ejecta of Nectarian basins and large craters equivalent to units Ioho and Ip with more erosional degradation.

Imbrian

Imbrian system: units, description, and interpretation (based on Unified Geologic Map of the Moon (1:5,000,000 scale) after Fortezzo et al. 2020, Figure 2b.

Ic; Imbrian Crater, Undivided; subdued topographic relief compared to younger impact features, usually less than 40 km in diameter, broad flat floors, and little to no ejecta present. Subdued morphology and material from a primary impact event.

Ic1; Imbrian Crater, Lower; similar to unit Ic, craters mantled by materials of the Orientale group; subdued morphology and material from a primary impact event, younger than Imbrium group materials but older than Orientale group materials.

Ic2; Imbrian Crater, Upper; similar to unit Ic, craters superpose materials of the Orientale group; subdued morphology and material from a primary impact event, younger than Orientale group materials but older than unit Im2.

Icc; Imbrian Crater, Catena; subdued and mantled elongated linear to elliptical clusters of circular and semi-circular depressions, usually overlapping; impact crater clusters derived ejecta from large, basin-forming impacts. Possibly primary impacts.

Isc; Imbrian Crater, Secondary; small diameter craters, densely spaced near and/or on the ejecta blanket of craters; impact crater forms derived from blocky material ejected from the primary impact.

Icf; Imbrian Crater, Fracture Floor; crater floors are typically domed, with furrows and/or linear to curvilinear fractures with highly variable widths and depths. Blocks and material between the fractures are locally reoriented; brittle materials uplifted and extended.

Ib; Imbrian Basin, Undivided; gently rolling into hilly terrain with aggregates of subdued irregular to circular craters. In addition, forms the outer basin and eject of crater Schrodinger; materials set during the formation of multi-ringed impact basins.

Ibm; Imbrian Basin, Massif; rugged blocks that form arcuate raised ridges within crater Schrodinger; material uplifted during basin formation, representing the inner ring of a multi-ringed impact basin.

Id; Imbrian Dark Mantle; some of the lowest albedo material mapped, usually near the outer margins of larger basins. Scalloped, smooth textures with small craters; pyroclastic material.

Ig; Imbrian Grooved; covers craters and other terrae of pre-Nectarian – Imbrian age. Craters have radial grooves on rims and walls with mounds. Origin: uncertain. Possibly Imbrium ejecta or a consequence of seismic shaking.

Iia; Imbrian Imbrium Alpes Formation; angular blocky and knobby with a smooth, mantled surface. Closely spaced hills and hummocks of 2–5 km in diameter; possibly eroded ejecta, structurally deformed bedrock, or both.

Iiap; Imbrian Imbrium Apenninus Formation; coarse blocks of material parallel to scarp bordering Imbrium basin. Smooth to undulating interblock materials; intensely fractured bedrock with interstitial Imbrium ejecta.

Iic; Imbrian Imbrium Crater; Individual craters <25 km diameter, clusters, and chains of craters up to 10 km in diameter, radial to Imbrium. Moderately subdued topographic features; secondaries and crater chains set during Imbrium basin formation.

Iif; Imbrian Imbrium Fra Mauro Formation; sinuous, curvilinear, and straight ridges draping the surface below. Surface texture locally hummocks; ejecta from the Imbrium basin and materials of the substrate.

Im1; Imbrian Mare, Lower; forms, flat, smooth surfaces. Relatively higher albedo compared to unit Im2 but lower albedo than unit Ip. A high density of superposed craters; old basaltic lava, probably of the same age as the Orientale basin.

Im2; Imbrian Mare, Upper; flat forms, smooth surfaces. Lower albedo and crater density than unit Im1. Numerous ridges. Difficult to distinguish from Id unit. Basaltic lava flows.

Imd; Imbrian Mare, Dome; abruptly sloping, high-relief, rough domical or conical shaped edifices, locally with pitted summits; volcanic edifices or laccoliths.

Iohi; Imbrian Orientale Hevelius Formation, Inner Facies; curvilinear to swirly ridges and troughs mostly radial and subradial to Orientale basin; continuous ejecta blanket set during outward flow of hot, turbulent, mobile materials.

Ioho; Imbrian Orientale Hevelius Formation, Outer Facies; swirly, lineated, hummocky, and smooth materials forming a discontinuous and irregular boundary; thinning distal margins of Orientale basin ejecta.

Ios; Imbrian Orientale Hevelius Formation, Secondary Crater Facies; overlapping crater chains and clusters radial and peripheral to the basin; secondary impact craters formed by ejected blocks.

Iom; Imbrian Orientale Maunder Formation; smooth to rolling, intensely fractured plains with broad linear ridges and smooth domes. Mostly impact melt. Ridges and domes are likely original floor material modified through compression.

Iork; Imbrian Orientale Montes Rook Formation, Knobby Facies; knobby, hummocky, rolling, and chaotic materials with interstitial irregular grooves and depressions; uppermost part of the overturned flap of the ejecta sequence of Orientale basin.

Iorm; Imbrian Orientale Montes Rook Formation, Massif Facies; high-relief, smooth blocks marking the second and third rings of the basin; structurally uplifted bedrock, thickly veneered with late arriving ejecta.

Ip; Imbrian Plains; smooth, flat to undulatory terrain of intermediate albedo occurring usually in topographic lows and crater floors of Imbrian and older age; ambiguous origin. Orientale and other large impact crater ejecta.

It; Imbrian Terra; low relief, low crater density, moderate to high albedo, moderately smooth surface; complex mixture of local erosional debris and crater and basin ejecta; megaregolith.

Itd; Imbrian Terra, Dome; outlines and characteristics similar to main-sequence craters, with smooth inner flanks, paucity of ejecta, inner terracing, secondary cratering; possibly target material differences or ash-flow calderas.

INp; Imbrian Nectarian Plains; smooth, flat to the undulating surface, moderate to high density of superposed craters; possibly materials emplaced by the formation of Imbrian and Nectarian basins.

INt; Imbrian Nectarian Terra; gently rolling terrain, moderate to high density of craters; complex mixture of local erosional debris, crater and basin ejecta; megaregolith.

Eratosthenian

Eratosthenian system: units, description, and interpretation (based on Unified Geologic Map of the Moon (1:5,000,000 scale) after Fortezzo et al. 2020, Figure 2c.

Ec; Eratosthenian Crater; non-rayed, circular craters with sharp to partially subdued crater rim crests, partial circumferential ejecta, lower albedo compared to unit Cc; morphology and material from a primary impact event.

Ecc; Eratosthenian Crater, Catena; elongated linear to elliptical clusters of circular to semi-circular depressions, often overlapping; impact crater clusters derived ejecta from large, basin-forming impacts. Possibly primary impacts.

Esc; Eratosthenian Secondary Crater; craters with small to very small diameter, densely spaced near and/or on the ejecta blanket of craters; impact crater forms derived from blocky material ejected from the primary impact.

Em; Eratosthenian Mare; low relative brightness plains with relatively few craters large enough to map, patches of small domes, sharp-crested ridges, observable flow fronts; relatively thin, young volcanic flows or pyroclastic material.

EIp; Eratosthenian Imbrian Plateau; High standing plateaus (relative to the mare surfaces in Oceanus Procellarum) with domes, cones, and dark mantling materials; volcanic constructs, flows, and pyroclastic materials.

Copernican

Copernican system: units, description, and interpretation (based on the Unified Geologic Map of the Moon (1:5,000,000 scale) after Fortezzo et al. 2020, Figure 2c.

Cc; Copernican Crater; rim, wall, and floor deposits with sharp rims, and circular to polygonal outlines. High relative brightness and rays; n/a.

Ccc; Crater, Catena; elongated linear clusters of overlapping circular to semi-circular; n/a.

Csc; Copernican Crater, Secondary; small to exceedingly small diameter craters, densely spaced near and/or on the ejecta blanket of craters; impact crater forms derived from blocky material ejected from the primary impact.

2. Lunar resources

The occurrence of mineral deposits on the moon based on the interpretation of rocket photography was first analyzed by Mueller et al. (Mueller et al. 1967). He suggested the volume and grade of the important metals and non-metallic minerals. Subsequent works, based on new data obtained from lunar satellites (Carpanter et al. 2016) and the lunar samples returned from lunar landing missions, allowed us to formulate conclusions about the resources present there (Heiken et al. 1991; Crawford 2015; Blair et al. 2002; Przylibski et al. 2022). These resources are associated with a surface layer known as regolith, the exploration of which is relatively good as it is based not only on remote surveys but also on collected samples (Wiśniewski et al. 2022). When it comes to minerals in lunar rocks, the degree of their exploration is insufficient and based on remote and geophysical surveys.

REE

Rare earth elements (including lanthanides) are a group of transition metals. A well-explored region of the Moon is the Procellarum KREEP Terrain, (PKT) (KREEP = potassium (K) + REE + phosphorus (P) (Warren and Wasson 1979; Wachowicz et al. 2019), Figure 3.

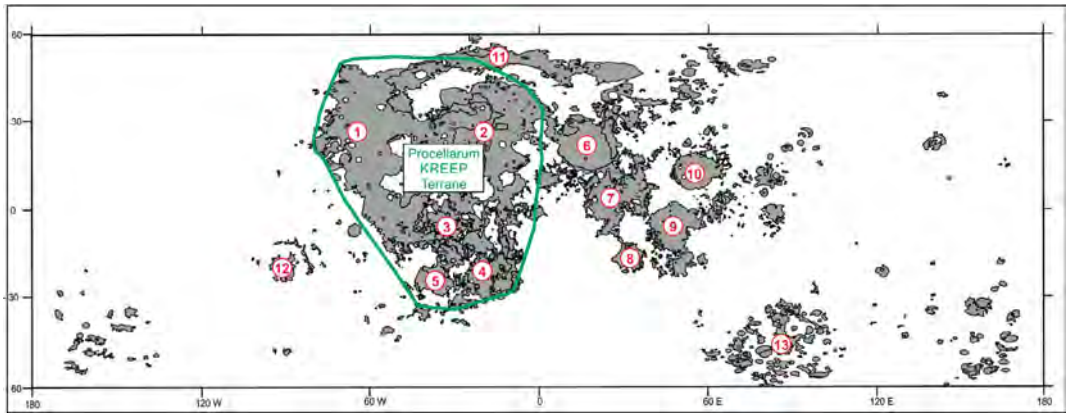

Fig. 3. Location of Procellarum KREP Terrane against the background of major oceanus and maria in the lunar area
1 – Oceanus Procellarum, 2 – Mare Imbrium, 3 – Mare Cognitum, 4 – Mare Nubium, 5 – Mare Humorum, 6 – Mare Serenitatis, 7 – Mare Tranquillitatis, 8 – Mare Nectaris, 9 – Mare Fecunditatis, 10 – Mare Crisium, 11 – Mare Frigoris, 12 – Mare Orientale, 13 – Mare Australe
after: United States Geological Survey (USGS), NASA Planetary Data System (PDS), Fortezzo et al. 2020

Rys. 3. Lokalizacja Procellarum KREP Terrane na tle głównych oceanów i mórz w obszarze księżycowym

It is possible to map the distribution of KREEP through the use of orbiting instruments able to detect gamma rays emitted by radioactive Th elements (Prettyman et al. 2006). KREEP-rich lithologies are generally related to Oceanus Procellarum and the Imbrium Basin on the north-western nearside (Jolliff et al. 2000). The total REE concentration is around 1,200 ppm (0.12 wt%); yttrium and cerium have concentrations of about 300 ppm each; however, europium and lutetium have concentrations of only 3–5 ppm (Warren and Wasson 1979).

Th and U

When it comes to lunar resources, U and Th are concentrated in KREEP-rich terrains (Yamashita et al. 2010), Figure 3. The maximum concentrations of these elements are 2.1 ppm for uranium and 7.3 ppm for thorium, recorded in the Copernicus crater. The South Pole-Aitken terrain (Jolliff et al. 2000) has higher abundances of the two mentioned elements than the adjacent areas.

Fe and Ti

The lunar maria Figure 3 are composed of basaltic lava flows. These basalts are relatively rich in Mg, Fe, and Ti, while relatively poor in Ca and Al. Iron (Fe) is abundant in all mare basalts at 14–17 wt%; (Papike et al. 1998), mostly in silicate minerals (e.g. pyroxene and olivine). The main oxide mineral containing Fe and Ti is ilmenite ($FeTiO_3$). Lunar basalts, due to their Ti content, are classified as 'low Ti' if their TiO_2 content is between 1–6 wt%, and 'high Ti' if their TiO_2 content is >6 wt% (Neal and Taylor 1992). The ilmenite-bearing high-Ti basalts are generally confined to two geographically restricted nearside mare regions (Oceanus Procellarum in the west and Mare Tranquillitatis in the east). High concentrations of metal oxides correspond to the South Pole Aitken basin (Lucey et al. 1998).

Aluminum

Another potentially useful metal is aluminum (Al); Al concentration in lunar regolith is 10–18 wt% (Lodders and Fegley 1998).

Silicon

Silicon (Si) is abundant in all rock types (about 20 wt% in lunar materials) (Stoeser et al. 2010).

Helium-3

The distribution of lunar He-3 (Fa and Jin 2007) is associated with 'high-Ti' basalts in the Oceanus Procellarum and Mare Tranquillitatis areas. In these two areas, covering a total of approximately 2 million km^2, He-3 concentrations may exceed 20 ppb. This is about five times the global average of 4.2 ppb determined by Fegley and Swindle (Fegley and Swindle 1993). Assuming a regolith thickness of 3 m, one can obtain a total He-3 mass for these two regions of approximately 2×10^8 kg.

Oxygen

The production of oxygen on the Moon using lunar soil, regolith or polar ice, is of specific interest, since oxygen can be used to sustain human life and as fuel (Crawford 2015; Hadler et al. 2019).

Conclusions

Generally, the geological exploration of the Moon can be considered to be relatively good. This is the result of magmatic interactions related to endogenous processes with impact structures. Endogenous processes are related to magma movements and differentiation during the cooling of the moon. Impact structures formed when the lunar surface was bombarded with space rocks of varying sizes. The largest were the size of asteroids and the smallest were the size of space dust. The entire lunar surface is covered with a relatively thin layer, usually several meters thick, the so-called regolith containing unsorted material consisting of dust and breccia. The maps shown in Figure 2 allow a chronological analysis of both structures and forms formed in the lunar area over the period from about 4.6 million years ago to the present day. The oldest structures –basins – have been covered over time by new structures known as mares, which are filled with basalts, now characterized by a low albedo. They are surrounded by high albedo plains, highlands, and mountain ("terra") areas. The entire area is covered with craters and accompanying structures formed during their formation.

The Moon's resource potential is usually considered in terms of its exploitation (International Space Exploration Coordination Group 2022) to obtain the raw materials needed on earth and its colonization. From the presented analysis, it appears that the rare earth elements (REEs) found in the KREEP area (Figure 3) currently appear to be the most prospective for extraction and transportation to earth. Their depletion on the earth is significant, and the demand is increasing because they are necessary for so-called high technologies. Another potential energy source for which the demand may increase is He-3. This could happen if the technology to produce energy through thermonuclear fusion is developed. At present, both REEs and He-3 can only be considered theoretically recoverable mainly due to the lack of appropriate technology and the extremely high costs of extracting them. Other raw materials such as Fe, Ti, Al, Si, U, Th, etc. should be considered as those that can be used to colonize the moon, build the infrastructure needed to do so, and produce oxygen and water, which are essential to human life.

This article was supported by research subvention AGH No 16.16.140.315.

REFERENCES

Baldwin, R.B. 1949. *The face of the Moon*. Chicago, University of Chicago Press, 239 p.

Baldwin, R.B. 1972. The tsunami model of the origin of ring structures concentric with large lunar craters. *Physics of the Earth and Planetary Interiors* 5(5), pp. 327–339.

Bills, B.G. and Ferrari, A.J. 1977. Alunar density model consistent with topographical, gravitational, librational, and seismic data. *Journal of Geophysical Research* 82(8), pp. 1306–1314.

Blair et al. 2002 – Blair, B.R., Diaz, J. and Duke M.B. 2002. Space Resource Economic Analysis Toolkit: The Case for Commercial Lunar Ice Mining. *Final Report to the NASA Exploration Team*, pp. 78.

Carpanter et al. 2016 – Carpenter, J., Fisackerly, R. and Houdou, B. 2016. Establishing lunar resource viability, *Space Policy* 37, pp. 52–57, DOI: 10.1016/j.spacepol.2016.07.002.

Cooper et al. 1974 – Cooper, M.R., Kovach, ILL. and Watkins, J.S. 1974. Lunar near-surface structure. *Reviews of Geophysics and Space Physics* 12(3), pp. 291–308, DOI: 10.1029/RG012i003p00291.

Crawford, I.A., 2015. *Lunar resources: A review, Progress in Physical Geography* 39(2), pp. 137–167, DOI: 10.1177/0309133314567585.

El-Baz, F. 1975. The Moon after Apollo. *Icarus* 25(4), pp. 495–537, DOI: 10.1016/0019-1035(75)90033-0.

Fa, W. and Jin, Y.Q. 2007. Quantitative estimation of helium-3 spatial distribution in the lunar regolith layer. *Icarus,* 190, pp. 15–23, DOI: 10.1016/j.icarus.2007.03.014.

Fegley, B. and Swindle, T.D. 1993. *Lunar volatiles: implications for lunar resource utilization*. [In:] Lewis, J., Matthews, M.S. and Guerrieri, M.L. (eds) *Resources of Near Earth Space*. Tucson: Tucson University Press, pp. 367–426.

Fortezzo et al. 2020 – Fortezzo, C.M., Spudis, P.D. and Harrel, S.L. 2020. Release of the Digital Unified Global Geologic Map of the Moon At 1:5,000,000 – Scale. Paper presented at the *51st Lunar and Planetary Science Conference*, Lunar and Planetary Institute, Houston, TX. [Online:] https://www.hou.usra.edu/meetings/lpsc2020/pdf/2760.pdf [Accessed: 2022-11-01].

Hadler et al. 2019 – Handler, K., Martin, D.J.P., Cilliers, J.J., Morse, A., Starr, S., Rasera, J.N., Seweryn, K., Reiss, P. and Meurisse, A. 2019. A universal framework for Space Resource Utilisation (SRU). *Planetary and Space Science* 182(23), DOI: 10.1016/j.pss.2019.104811.

Heiken et al. 1991 – Heiken, G.H., Vaniman, D.T., French, B.M. 1991. *Lunar Sourcebook*. Cambridge University Press, pp.778. [Online:] https://ntrs.nasa.gov/api/citations/20160013682/downloads/20160013682.pdf [Accessed: 2022-11-01].

International Space Exploration Coordination Group 2022 – *The Global Exploration Roadmap – Supplement August 2022: Lunar Surface Exploration Scenario Update*, ISECG.

Jolliff et al. 2000 – Jolliff, B.L., Gillis, J.J., Haskin, L.A., Korotev, R.L. and Wieczorek, M.A. 2000. Major lunar crustal terranes: Surface expressions and crust-mantle origins. *Journal of Geophysical Research – Planets* 105(E2), pp. 4197–4216, DOI: 10.1029/1999JE001103.

Kaula et al. 1973 – Kaula, W.M., Schubert, G., Lingenfelter, R.E., Sjogren, W.L. and Wollenhaupt, W.R. 1973. Lunar topography from Apollo 15 and 16 laser altimetry. *Proceedings of the Lunar Science Conference* 4, pp. 2811–2819.

Lodders, K. and Fegley, B. 1998 – *The Planetary Scientist's Companion*. Oxford: Oxford University Press.

Lucey et al. 1998 – Lucey, P.G., Taylor, G.J. and Hawke, B.R. 1998. FeO and TiO_2 concentrations in the South Pole–Aitken basin: implications for mantle composition and basin formation. *Journal of Geophysical Research – Planets* 103(E2), pp. 3701–3708, DOI: 10.1029/97JE03146.

Mueller, G. 1967. Mineral Deposits on the Moon. *Nature* 215, pp. 1149–1151.

Neal, C.R. and Taylor, L.A. 1992. Petrogenesis of mare basalts. A record of lunar volcanism. *Geochimica et Cosmochimica Acta* 56: pp. 2177-2211.

Neukum, G. and Ivanov, B. A. 1994. Crater size distributions and impact probabilities on Earth from lunar, terrestrial – planet, and asteroid cratering data. [In:] *Hazard Due to Comets and Asteroids*. Univ. of Ariz. Press, Tucson pp. 359–416.

Papike et al. 1998 – Papike, J.J., Ryder, G. and Shearer, C.K. 1998. Lunar samples. *Reviews in Mineralogy and Geochem*istry 36, pp. 5.1–5.234.

Prettyman et al. 2006 – Prettyman, T.H., Hagerty, J.J., Elphic, R.C., Feldman, W.C., Lawrence, D.J., McKinney, G.W. and Vaniman, D.T. 2006. Elemental composition of the lunar surface: Analysis of gamma-ray spectroscopy data from Lunar Prospector. *Journal of Geophysical Research* 11(E12), DOI: 10.1029/2005JE002656.

Przylibski et al. 2022 – Przylipski, T.A., Łuszczek, K., Blutstein, K., Szczęśniewicz, M. and Ciapka, D. 2022. Extraterrestrial mining in Poland (*Górnictwo pozaziemskie w Polsce*). *Przegląd Górniczy* 3, pp. 17–24 (*in Polish*).

Shoemaker, E.M. and Hackman, R.J. 1962. *The Moon.* Academic Press, N.Y., p. 289.

Shoemaker et al. 1967 – Shoemaker, E.M., Batson, R.M., Holt, H.E., Morris, E.C., Rennilson, J.J. and Whitaker, E.A. 1967. Iblevision observations from Surveyor 111/3 of Surveyor 111: *A preliminary report: NASA Report SP-146,* pp. 9–59.

Shoemaker, E.M. and Morris, E.C. 1970. *Geology*: Physics of fragmental debris. *Icarus* 12(2), pp. 188–212.

Stoeser et al. 2010 – Stoeser, D., Wilson, S. and Rickman, D. 2010. Design and specifications for the highland regolith prototype simulants NU-LHT-1M and -2M. *NASA Technical Report TM-2010-216438*.

Stöffler, D. and Ryder, G. 2001. Stratigraphy and isotope ages of lunar geologic units: Chronological standard for the inner solar system. *Space Science Reviews* 96(1/4), pp. 9–54, DOI: 10.1023/A:1011937020193.

Toksoz et al. 1974 – Toksoz, M.N., Dainty, A.M., Solomon, S.C. and Anderson, K.R., 1974. Structure of the Moon. *Reviews of Geophysics and Space Physics* 12(4), pp. 539–567.

van Gasselt, S. and Neukum, G. 2011. *Chronology, Cratering and Stratography*. [In:] *Encyclopedia of Astrobiology*. Springer, Berlin, Heidelberg, DOI: 10.1007/978-3-642-11274-4_294.

Wachowicz et al. 2019 – Wachowicz, M.E., Frąk, P., Węgłowski, A., Burdzy, Z., Bachtin, R., Bankiewicz, J. and Gołąbek, W. 2019. *Space Mining Challenges: Expertise of the Polish Entities and International Perspective on Future Exploration Missions*. [In:] Sasiadek, J. (eds) *Aerospace Robotics III. GeoPlanet: Earth and Planetary Sciences*. Springer, pp. 212, DOI: 10.1007/978-3-319-94517-0_10.

Warren, P.H. and Wasson J.T. 1979. The origin of KREEP. *Reviews of Geophysics and Space Physics* 17, pp. 73–88.

Wilhelms, D.E. 1987. *The geologic history of the Moon*. U.S. Geol. Surv. Prof. Pap., 302 pp., DOI: 10.3133/pp1348.

Wiśniewski et al. 2022 – Wiśniewski, Ł., Wasilewski, G., Kędziora, B. and Grygorczuk, J. 2022. Wybrane właściwości regolitu i ich istotny wpływ na realizację misji eksploracyjnych (*Wybrane właściwości regolitu i ich istotny wpływ na realizację misji eksploracyjnych*). *Acta Societatis Metheoriticae Polonorum* 13, pp. 107–119 (*in Polish*).

Yamashita et al. 2010 – Yamashita, N., Hasebe, N., Reedy, R.C., Kobayashi, S., Karouji, Y., Hareyama, M., Shibamura, E., Kobayashi, M.N., Okudaira, O., D'Uston, C., Gasnault, O., Forni, O. and Kim, K.J. 2010. Uranium on the Moon: Global distribution and U/Th ratio. *Geophysical Research Letters* 37(10), L10201, DOI: 10.1029/2010GL043061.

GEOLOGICAL EXPLORATION OF THE MOON

Keywords

moon, geology, mineral deposits

Abstract

The earliest studies of the Moon consisted of observations from Earth and meteorites containing lunar material. As technology progressed, the observations were made using remote sensing techniques. The next stage of the Moon reconnaissance consisted of unmanned flights, and later manned flights, with the help of which, in-situ tests were performed. The obtained materials enable the formulation of conclusions both about the geological structure and the mineral resources of the moon.

The latest maps provided by the United States Geological Survey (USGS) and NASA Planetary Data System (PDS) enable a detailed analysis of the geological structure of the moon. Since they are available in shapefile format for QGIS and ArcGIS software, they can be freely modified and processed. On the basis of these, it is possible to analyze the complexity of the geological structure of the moon, especially with regard to the structure of its substrate and the surface covered with craters. Data obtained from the observation of the Moon with the use of research satellites and research carried out during landings related to the collection of samples enabled the formulation of conclusions about the raw materials present there. These raw materials are related to the surface layer of the so-called regolith, the recognition of which is relatively good because it is based not only on remote studies but also on the basis of collected samples. Additionally, there are indications of the possible presence of mineral resources related to the substrate, but its recognition is relatively poor because it is based on remote and geophysical surveys. The presented analysis shows that the Moon has such minerals as rare earth elements (REE) and Th and U found in the KREEP area. Fe and Ti are found to be in basaltic lava flows occurring in the mares and aluminum, silicon and Helium-3 occur in the regolith.

STAN ROZPOZNANIA GEOLOGICZNEGO I ZŁOŻOWEGO KSIĘŻYCA

Słowa kluczowe

księżyc, geologia, surowce mineralne

Streszczenie

Najstarsze badania Księżyca polegały na jego obserwacjach z Ziemi oraz meteorytów zawierających materiał księżycowy. W miarę postępu technicznego obserwacje odbywały się za pomocą technik teledetekcyjnych. Kolejnym etapem rozpoznania Księżyca były loty początkowo bezzałogowe, a później załogowe, za pomocą których wykonano badania in situ. Pozyskane materiały pozwalają wnioskować zarówno o budowie geologicznej, jak i zasobach mineralnych Księżyca. Najnowsze mapy udostępnione przez United States Geological Survey (USGS) oraz NASA Planetary Data System (PDS) pozwalają na szczegółową analizę budowy geologicznej Księżyca. Ponieważ udostępnione są w formacie shapefile dla oprogramowania QGIS i ArcGIS, można je dowolnie modyfikować i przetwarzać. Na ich podstawie można analizować złożoność budowy geologicznej Księżyca zwłaszcza w odniesieniu do budowy jego podłoża oraz powierzchni pokrytej kraterami. Dane uzyskane z obserwacji Księżyca za pomocą satelitów badawczych oraz badań wykonanych podczas lądowań związanych z poborem próbek, pozwoliły na sformułowanie wniosków o występujących tam surowcach. Surowce te związane są z warstwą powierzchniową tzw. regolitem, którego rozpoznanie jest stosunkowo dobre, ponieważ opiera się nie tylko na badaniach zdalnych, ale i na podstawie pobranych próbek. Istnieją również przesłanki o możliwości występowania surowców mineralnych związanych z podłożem, jednak jego rozpoznanie jest stosunkowo słabe, ponieważ opera się na badaniach zdalnych i geofizycznych. Z przedstawionej analizy wynika, że na Księżycu występują takie surowce mineralne jak pierwiastki ziem rzadkich (REE) oraz Th i U występujące na obszarze KREEP. Fe i Ti występują w bazaltach budujących morza księżycowe oraz aluminium, krzem i hel-3 występują w regolicie.